HIGH-HARMONIC GYROTRON OSCILLATORS AND GYRO-KLYSTRON AMPLIFIERS

D.B. McDermott, D.S. Furuno, and N.C. Luhmann, Jr.

UCLA, Electrical Engineering Department

Los Angeles, California

ABSTRACT

The design and performance of several millimeter-wave harmonic gyrotron concepts are described in which the interaction is between axis-encircling electrons and cylindrical cavity TE_{n11} modes. This allows the magnetic field of the gyrotron to be reduced by an order of magnitude. Efficiencies up to 15% have been measured for moderate harmonic interactions, multi-kW power levels have been attained at the eleventh harmonic of the cyclotron frequency, 65 GHz waves have been produced, and a sixth-harmonic gyro-klystron amplifier has yielded 23 dB gain. Also, an 18 GHz, ½ MW fourth-harmonic gyrotron has been constructed and is being tested.

INTRODUCTION

Considerable effort is being devoted to the development of moderate-to-high power millimeter-wave sources. The gyrotron with electron orbits shown in Fig. 1a has proven to be an efficient source of high power, high frequency microwave radiation[1]. However, very high magnetic fields are required to produce millimeter waves, since the output frequency is comparable to the relativistic cyclotron frequency, $\Omega_c = eB/\gamma mc$, where $\gamma = (1-v\cdot v/c^2)^{-\frac{1}{2}}$, and v represents the electron velocity. Unfortunately, many of the applications preclude the use of both high field pulsed magnets and superconducting magnets. Another approach must be developed which can efficiently operate at high efficiency with low magnetic fields.

An alternate interaction is being developed at UCLA based on the synchronism between axis-encircling electrons and a high order TE_{n11} mode[2] where n represents the azimuthal mode number. The electron orbits in the new configuration are shown in Fig.1b. Synchronism exist between the electrons and cavity wave when $\omega = n\Omega_c$ and rf generation due to the negative mass instability occurs when $\omega \geq n\Omega_c$. The efficiency of this harmonic gyrotron interaction has been shown[3] to have the same parametric dependence as the conventional gyrotron. Therefore, the magnetic field requirements are reduced by a factor of n and the potential for very high efficiency still exists.

Because the TE_{n11} modes are strongly localized near the wall, the filling factor, which measures the strength of the interaction and is shown in Fig.2, peaks for high energy electrons. This would appear to necessitate the use of extremely bulky high voltage insulation. However, by the use of gyro-resonant rf-acceleration a compact system can be achieved. An rf cavity accelerator driven by a conventional high power microwave source can produce 500 keV rotating beam with currents up to 1A[4].

OSCILLATORS

RF-Acceleration

The basic cavity configuration is shown in Fig.3. A low energy, magnetized pencil electron beam is injected into the circularly polarized TE_{111} accelerated cavity. We presently have two operational systems; one is driven by a 200 kW, 9 GHz magnetron and the other is driven by a 1 MW, 3 GHz klystron amplifier. Both systems yield 500 keV electrons. The rotating electron beam then progresses through the gyrotron cavity and finally impacts with a diagnostic fluorescent Uranium glass witness plate, which yields $r_\perp$ (or γ).

The dependence of power and efficiency on current for the $TE_{11,1,6}$ interaction of Tube #S.3 is shown in Fig.4. Saturation occurs for beam currents one order of magnitude beyond the start of oscillation. The peak conversion efficiency of 2%, which is twice the output efficiency for the critically coupled interaction, is less than the theoretical prediction of 4%. However, in another experiment, 15% conversion efficiency was achieved in a third harmonic interaction.

The experimental start-oscillation current for the seventh and eighth harmonic interactions in an E-band cavity are plotted in Fig.5 as a function of magnetic field together with the theoretical start-oscillation curves. Good agreement exists with theory. 60W were emitted at 56 GHz and 12W at 65 GHz. Furthermore, since the initial cavity was undercoupled, a future critically coupled experiment should increase the power levels by an order of magnitude.

To obtain higher frequency output one must use either a higher order harmonic or a higher frequency accelerator driver. We have begun construction of a 50 kW, 35 GHz accelerator system which should yield 100-300 GHz radiation at 1 kW power levels.

Electrostatic Acceleration

As can be seen in Fig.2, the filling factor for moderate harmonic interactions is non-negligible for electron energies achievable by electrostatic acceleration at moderate voltages (75 kV, v/c =0.5). We have finished construction and begun testing a

0149-645X/84/0000-0187 $01.00 © 1984 IEEE

very high power (½ MW), fourth-harmonic gyrotron. The first model was designed to emit at 18 GHz. The rotating beam is produced by passing an annular beam through a magnetic cusp(5) as shown in Fig.6. The start-oscillation currents for a future ½ MW, 90 GHz tube are shown in Fig.7.

Dielectric Loading

An exciting novel concept under study is to increase the filling factor of the rotating e-beam with the radiation field by the insertion of a dielectric rod along the bore of the cavity(6), thereby allowing Neumann function solutions in the vacuum region. The filling factor can be made to peak for 80 keV electrons as shown in Fig.8 in a radical departure from the standard high-harmonic interaction. Here, the electrons interact with the evanescent field of a dielectric mode. The paramount experimental problems are 1)heat dissipation in the dielectric, 2)alignment accuracy, 3)coupling of the rf energy, and 4)surface charging of the rod. This concept has important ramifications for an electrostatically-accelerated high-harmonic gyrotron.

GYRO-KLYSTRON AMPLIFIER

The majority of microwave applications require an amplifier rather than an oscillator. A gyro-klystron amplifier which has been designed for operation at the sixth-harmonic is shown in Fig.9. This tube's gain characteristics are shown in Fig. 10 together with theoretical predictions. The peak small-signal gain of 23 dB is far in excess of theory suggesting that the drift tube is acting as a "third cavity". A saturation study is now underway. The peak output power should be 10 kW.

ACKNOWLEDGEMENT

The work was supported by U.S. Army Research Office Contract #DAAG29-82-K-0004 and U.S. Air Force Office of Scientific Research Grant #81-0200.

REFERENCES

(1) J.L. Hirshfield and V.L. Granatstein, IEEE Trans. MTT-25, 522 (1977).

(2) D.B. McDermott, N.C. Luhmann, Jr., D.S. Furuno, and A. Kupiszewski, Int. J. Infrared and Millimeter Waves 4, 639 (1983).

(3) D.B. McDermott, N.C. Luhmann, Jr., A. Kupiszewski, and H.R. Jory, Phys. Fluids 26, 1936 (1983).

(4) H.R. Jory and A.W. Trivelpiece, J. Appl. Phys. 39, 3053 (1968).

(5) W.W. Destler, R. Kulkarni, C.D. Striffler, and R.L. Weiler, J. Appl. Phys. 54, 4152 (1983).

(6) D.B. McDermott, D.S. Furuno, and N.C. Luhmann, Jr., Int. J. Infrared and Millimeter Waves 4, 831 (1983).

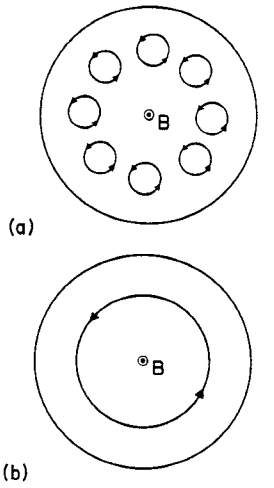

Figure 1. Schematic of electron trajectories in the (a) small-orbit, high magnetic field, standard gyrotron and in the (b) large orbit, low magnetic field, harmonic gyrotron.

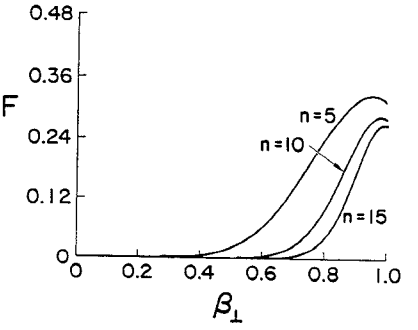

Figure 2. Dependence of the filling factor on $\beta_\perp$ for three high harmonic interactions.

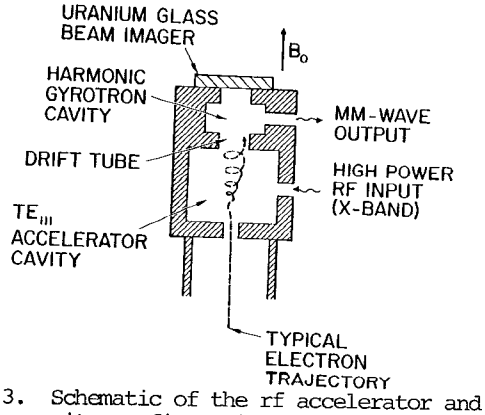

Figure 3. Schematic of the rf accelerator and gyrotron cavity configuration.

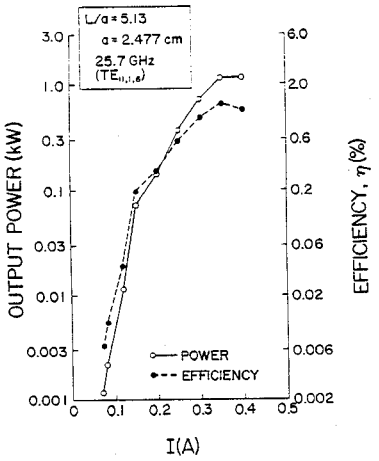

Figure 4. Dependence of eleventh harmonic output power and rf conversion efficiency on injected electron current for Tube #S.3.

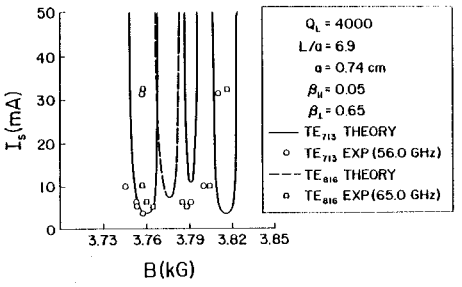

Figure 5. Experimental (data points) and theoretical (smooth curve) start-oscillation current as a function of magnetic field for Tube #X.5.

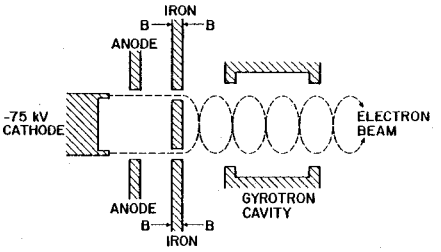

Figure 6. Schematic of electrostatic high-harmonic gyrotron system with e-gun, magnetic cusp, and interaction cavity.

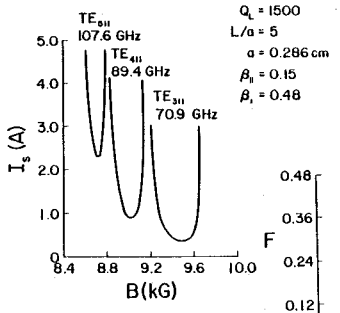

Figure 7. Theoretical start-oscillation current as a function of magnetic field for the third, fourth and fifth harmonic interactions in Tube #E.4.

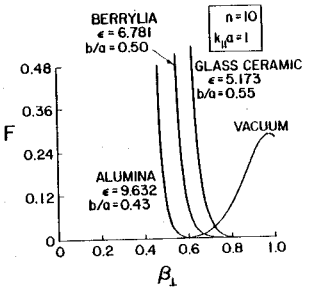

Figure 8. The dependence of the filling factor on $\beta_\perp$ for the lowest order modes in a berrylia, alumina, and glass ceramic rod for a tenth harmonic interaction. Also shown is the vacuum case.

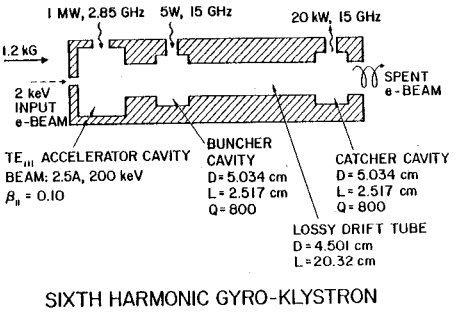

Figure 9. Schematic of the sixth harmonic gyro-klystron amplifier.

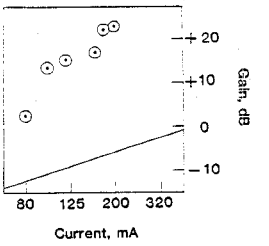

Figure 10. Gyro-klystron gain as a function of current for the sixth harmonic, 15 GHz, TE_{611} interaction.